Model Predictive Control Strategies for DC-DC Boost Voltage Conversion

Petros Karamanakos[1], Georgios Papafotiou[2], Stefanos Manias[1]
1* NATIONAL TECHNICAL UNIVERSITY OF ATHENS (NTUA)
Heroon Polytechniou 9
15780 Zografou-Athens, Greece
Tel.: +30 / 210 – 772.22.33.
Fax: +30 / 210 – 772.35.93.
E-Mail: petkar@central.ntua.gr, manias@central.ntua.gr
URL: http://www.ntua.gr
2* ABB CORPORATE RESEARCH
Segelhofstrasse 1K
5405 Baden-Daetwill, Switzerland
Tel.: +41 / 058 – 586.82.53.
Fax: +41 / 058 – 586.73.65.
E-Mail: georgios.papafotiou@ch.abb.com
URL: http://www.abb.com

Keywords

«Converter control», «Non-linear control», «Optimal control».

Abstract

This paper proposes a Model Predictive Control (MPC) for the boost dc-dc converter. Based on the state space description of the converter, a constrained optimal problem is formulated and solved. By regulating the current of the power circuit's inductor to a proper reference, set by an outer loop based on an observer, the main control objective, which is the regulation of the output voltage at a reference value, is achieved despite changes in the input voltage and the load. Experimental results are presented to verify the controller's feasibility and performance.

Introduction

The problems associated with dc-dc conversion power electronic topologies and their closed-loop controlled operation have been thoroughly studied in the past, resulting in a plethora of academic papers and a mature application environment in industry. However, the emergence of new applications with more demanding performance requirements, coupled with today's ability to employ novel computational control techniques due to affordability of more powerful control platforms, still motivate a number of research activities in the area. In this paper, we present some recent work done in the use of Model Predictive Control (MPC) for the control of boost dc-dc converter topologies. Specifically, we investigate a new control problem formulation for the simple boost converter (shown in Fig. 1), while the subsequent steps of our research will comprise its extension to interleaved topologies.

MPC has been successfully applied in complex control problems in the process industry, where it currently represents the state of the art [1], and its use has been expanding in the automotive [2] and power electronics industry. Although in the latter the employed MPC formulations have been rather elementary (see [3] and [4]), the method has already demonstrated a significant potential in achieving important performance improvements (see [5] and [6]), which can in many cases overshadow the less favorable features of the method, such as its increased computational complexity.

Regarding the material presented in this paper, on a first level, the control method introduced looks rather typical, since it comprises the usual two loops that are commonly employed in the operation of a

boost dc-dc converter: namely a current loop that drives the converter current to a specified reference, and an outer loop that sets this reference in such a way that the output voltage is regulated to a desired value. A closer look, however, reveals the differences: the inner current control regulation problem is posed in the MPC framework, while the outer loop is based on the estimation of the load current and the subsequent derivation of the inductor current reference using a simple power balance mathematical expression. More specifically, the inner current control loop is formulated using hysteresis bounds for the inductor current, which are modeled in the MPC framework using soft constraints, essentially borrowing on the approach introduced in [1], [5] and [6].

The benefits arising from this approach are of course the very fast current dynamics that MPC can deliver, combined with the inherent very good robustness properties of the method. Moreover, the use of longer prediction horizons, although not offering too much in the present setting, is expected to improve the controller's performance in terms of current sharing when extended to the interleaved topologies. On the other hand, the absence of a modulator and the direct manipulation of the converter switches imply a variable switching frequency. In the course of this work, we will explore the tradeoffs arising between the variation of the switching frequency (and the associated drawbacks) and the robustness and speed of control response that the proposed formulation can bring.

Mathematical model

The DC-DC boost converter (Fig. 1) is expressed in continuous time state space by the following equations [7]

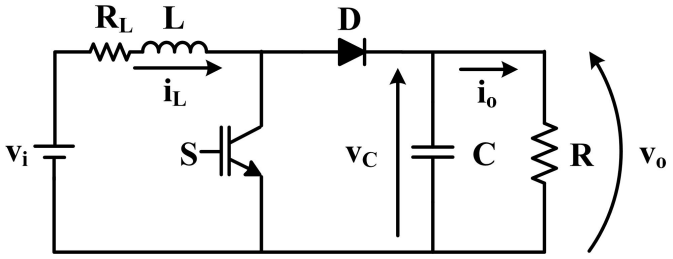

Fig. 1: DC-DC boost converter.

$$\frac{dx(t)}{dt} = \left(A_1 + A_2 \cdot u(t)\right) \cdot x(t) + B \cdot w(t) \tag{1}$$

$$y(t) = C \cdot x(t) \tag{2}$$

where

$$x(t) = \left[i_L(t) \;\; v_o(t)\right]^T, A_1 = \begin{bmatrix} -\frac{R_L}{L} & -\frac{1}{L} \\ \frac{1}{C} & 0 \end{bmatrix}, A_2 = \begin{bmatrix} 0 & \frac{1}{L} \\ -\frac{1}{C} & 0 \end{bmatrix}, B = \begin{bmatrix} \frac{1}{L} & 0 \\ 0 & -\frac{1}{C} \end{bmatrix}, w(t) = \left[v_i(t) \;\; i_o(t)\right]^T,$$

$$C = \begin{bmatrix} 0 & 1 \end{bmatrix}$$

where C the filter capacitance, L the circuit inductance, R_L the internal resistance of the inductor, $i_L(t)$ the inductor current (equal to the input current), $i_o(t)$ the load current, $v_o(t)$ the output voltage, and $v_i(t)$ the input voltage. Given the input voltage $v_i(t)$, the output $v_o(t)$ should be regulated at some desired value with suitable choice of control, which means by appropriate switching. Finally the variable u defines the switching position:

$$u = \begin{cases} 1, \ switch \rightarrow on \\ 0, \ switch \rightarrow off \end{cases} \tag{3}$$

In order to design and apply the MPC strategy, the developed continuous-time state space mathematical model is discretized using first-order approximation. This leads to the following discrete-time state space model, defined as

$$x(k+1) = \left(A_{1,d} + A_{2,d} \cdot u(k) \right) \cdot x(k) + B_d \cdot w(k) \tag{4}$$

$$y(k) = C_d \cdot x(k) \tag{5}$$

where

$$x(k) = \left[I_L(k) \ V_o(k) \right]^T, \ A_{1,d} = (I + A_1 \cdot T_s) = \begin{bmatrix} 1 - \frac{R_L}{L} T_s & -\frac{T_s}{L} \\ \frac{T_s}{C} & 1 \end{bmatrix}, \ A_{2,d} = A_2 \cdot T_s = \begin{bmatrix} 0 & \frac{T_s}{L} \\ -\frac{T_s}{C} & 0 \end{bmatrix},$$

$$B_d = B \cdot T_s = \begin{bmatrix} \frac{T_s}{L} & 0 \\ 0 & -\frac{T_s}{C} \end{bmatrix}, \ w(k) = \left[V_i(k) \ I_o(k) \right]^T, \ C_d = C = \left[0 \ 1 \right], \ u(k) = u$$

where capital letters denote the discrete time-varying physical quantities, and T_s the sampling time.

Controller design

In this section the design of the nominal controller is presented. Firstly an objective function is formulated. Following, this function is minimized based on an optimal state-feedback control law, subjected to hard and/or soft constraints. Furthermore, disturbances, such as inductor resistance and load current uncertainties, are taken into account. Thus, the controller is augmented by a second order Luenberger observer in order to address unmeasured changes in the load, while the way that the inductor resistance uncertainty affects the inductor current is shown.

Nominal controller design

Given the input voltage $v_i(t)$, the output $v_o(t)$ should be regulated at some desired value with suitable choice of the control action, which means by appropriate switching. The main control objective is to act on the switching semiconductor appropriately, in order to achieve an output voltage equal to its reference, despite changes in the input voltage and the load.

The procedure of MPC is the following: With respect to the system dynamics and the problem's constraints, an objective function is designed, subjected to hard and/or soft constraints. Then the control action is obtained by minimizing the objective function, at each step, over a finite prediction horizon, which recedes by one sampling interval respectively (receding horizon strategy) [1].

As already mentioned, MPC is used for the inner current control regulation problem by using hysteresis bounds for the inductor current. These bounds are defined by the maximum and minimum values of the reference inductor current, added in the controller as soft constraints. Thus, a slack variable $e(k)$ is introduced, intended to capture the degree of violation of the inductor current constraints which are weighted with p_a and $p_b \in R^+$ ([1], [5] and [6]).

$$e(k)=\begin{cases} p_a \cdot \left(I_L(k)-I_{L,\max}\right) & if\ I_L(k)\geq I_{L,\max} \\ p_a \cdot \left(I_{L,\min}-I_L(k)\right) & if\ I_L(k)\leq I_{L,\min} \\ p_b \cdot \left|I_L(k)-I_L^*\right| & else \end{cases} \tag{6}$$

where the terms $I_{L,max}$ and $I_{L,min}$ are specified as a percentage of the reference I_L^*.

Considering all the errors mentioned by (6), an objective function which penalizes the error's evolution over the finite horizon N is introduced (see [5] and [6])

$$J(k)=\sum_{n=1}^{N}\left\|e(k+n\,|\,k)\right\|_1 \tag{7}$$

The control input is then achieved by minimizing in each sampling period the objective function (7) subjected to constraints

$$\begin{aligned} &u^*(k) \;=\; min\, J(k) \\ &subject\ to\ eq.\ (4),\ (5)\ and\ (6) \end{aligned} \tag{8}$$

In order to manipulate the reference inductor current, and assuming in a first approximation that the power switches are ideal, the equality of the input and output power of the boost converter, $P_{in} = P_{out}$, is taken into account

$$I_L^* = \frac{V_i}{2\cdot R_L} - \sqrt{\left(\frac{V_i}{2\cdot R_L}\right)^2 - \frac{V_o^*\cdot I_o}{R_L}} \tag{9}$$

Disturbances

Inductor resistor uncertainty

In the power balance equation the resistance of the inductor is not neglected, although its value is considered constant. Due to this approximation, an error between the calculated reference value of the inductor current and the actual desired reference value is expected [8]. This error can be calculated by the power balance equation, if the increase of the inductor resistance value is taken into account.

As mentioned above, in equation (9) the internal resistance of the inductor, R_L, is rated as constant. In reality, though, the value of the resistance increases as the temperature increases. The contribution of the change of the resistance to the reference inductor current is given by

$$\frac{dI_L^*}{dR_L} = -\frac{V_i}{2\cdot R_L^2} + \frac{V_o\cdot I_o}{R_L\cdot\sqrt{V_i^2-4\cdot R_L\cdot V_o\cdot I_o}} + \frac{\sqrt{V_i^2-4\cdot R_L\cdot V_o\cdot I_o}}{2\cdot R_L^2} \tag{10}$$

Fig. 2a shows the rate of change of the reference inductor current in respect to the resistance of the inductor, which changes from its nominal value (0.37 Ohm) to a 50% increase, while the converter operates under input voltage equal to 15.5 V, output voltage 40 V, and two different ohmic loads (R_1 = 73 Ohm and R_2 = 35 Ohm). In Fig. 2b the percentage of the change of the inductor current under the same operating points is depicted.

The output voltage of the converter (which in this work is controlled by controlling the inductor's current) is connected to the inductor's current via the above equation [8]

$$V_o = (1-D)\cdot R\cdot I_L^* \tag{11}$$

where R stands for the ohmic load, and D is the duty cycle (t_{on}/T_s, where t_{on} is the interval the switching semiconductor operates and T_s the switching period). Due to the fact that the converter operates under variable switching period, the duty cycle can be approximately calculated, under a "window" which includes many switching periods, by the following equation

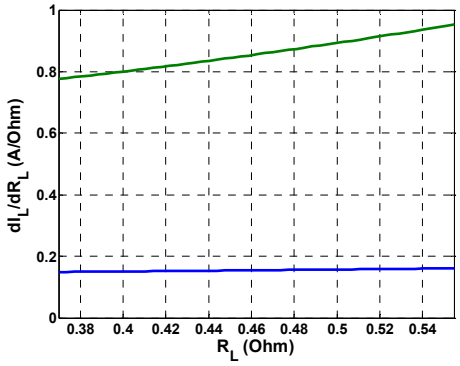

(a) Rate of change of the reference inductor current in respect to the inductor's resistance. (Blue line corresponds to R=73 Ohm, green line corresponds to R=35 Ohm)

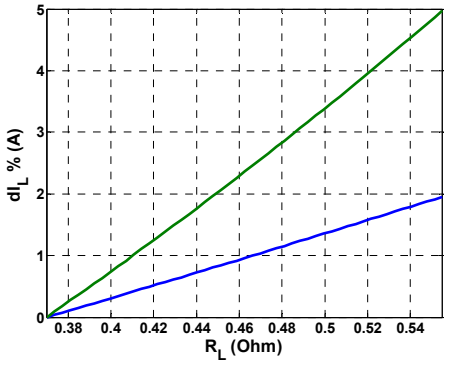

(b) Per cent change of the inductor current in respect to the inductor's resistance. (Blue line corresponds to R=73 Ohm, green line corresponds to R=35 Ohm)

Fig. 2. Contribution of the change of the resistance to the reference inductor current.

$$D = 1-\left(\frac{V_i}{2\cdot V_o}+\sqrt{\left(\frac{V_i}{2\cdot V_o}\right)^2-\frac{R_L}{R}}\right) \tag{12}$$

The contribution of the change of the resistance to the output voltage is equal to

$$\frac{dV_o}{dR_L} = \frac{d((1-D)\cdot R\cdot I_L^*)}{dR_L} \tag{13}$$

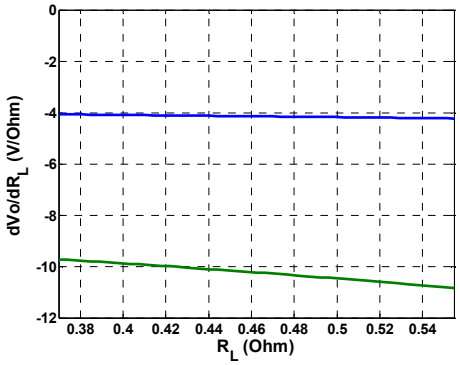

(a) Rate of change of the output voltage in respect to the inductor's resistance (Blue line corresponds to R=73 Ohm, green line corresponds to R=35 Ohm)

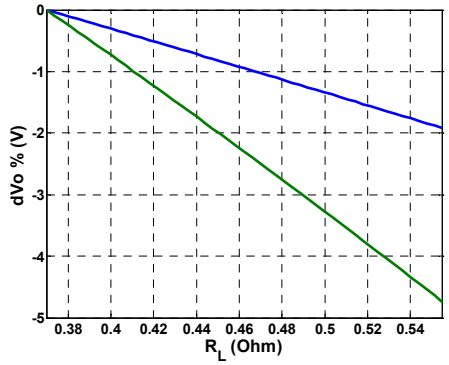

(b) Per cent change of the output voltage in respect to the inductor's resistance. (Blue line corresponds to R=73 Ohm, green line corresponds to R=35 Ohm)

Fig. 3. Contribution of the change of the resistance to the output voltage.

Fig. 3a shows the rate of change of the output voltage in respect to the resistance of the inductor, which changes from its nominal value (0.37 Ohm) to a 50% increase, while the converter operates under the operating points mentioned above. In Fig. 3b the percentage of the change of the output voltage under the same operating points is depicted.

Figs. 2 and 3 show that due to the increase of the inductor resistance the error in the calculation of the reference inductor current, and the corresponding error in the output voltage, is not negligible, especially for smaller loads. In order to alleviate this error an observer which would be able to take into consideration the inductor current disturbances, such as a discrete-time Kalman filter [9], could be introduced. In such a way the deviations from the nominal value of the inductor resistance would be taken into account, since the effect of the changing inductor resistance on the inductor current is modeled.

Load current uncertainty

Due to the fact that the load could be a variable resistor, or as in most of the cases, a non linear load, such as a power converter, a second order Luenberger observer is designed [10] for estimating instead of measuring the load current. By this, the design of the controller is decoupled from the type and the value of the load, while the hardware cost is reduced.

From the circuit analysis the current equation is the following

$$i_{diode} = i_C + i_o \Leftrightarrow i_C = (1-u)\cdot i_L - i_o \Leftrightarrow \frac{dv_o}{dt} = \frac{i_L}{C}\cdot(1-u) - \frac{i_o}{C} \tag{14}$$

The output dynamics are given in continuous time state space by

$$\frac{dx_L(t)}{dt} = A_L \cdot x_L(t) + B_L \cdot \bar{u}(t) \tag{15}$$

$$y_L(t) = C_L \cdot x_L(t) \tag{16}$$

where

$$x_L(t) = \begin{bmatrix} i_o(t) & v_o(t) \end{bmatrix}^T,\ \bar{u}(t) = 1-u(t),\ A_L = \begin{bmatrix} 0 & 0 \\ -\frac{1}{C} & 0 \end{bmatrix},\ B_L = \begin{bmatrix} 0 & \frac{i_L(t)}{C} \end{bmatrix}^T,\ C_L = \begin{bmatrix} 0 & 1 \end{bmatrix}$$

The above continuous time state space system can be discretized by using first-order approximation

$$x_L(k+1) = A_{L,D} \cdot x_L(k) + B_{L,D} \cdot \bar{u}(k) \tag{17}$$

$$y_L(k) = C_{L,D} \cdot x_L(k) \tag{18}$$

where

$$x_L(k) = \begin{bmatrix} I_o(k) & V_o(k) \end{bmatrix}^T,\ \bar{u}(k) = 1-u(k),\ A_{L,D} = (I + A_L \cdot T_s) = \begin{bmatrix} 1 & 0 \\ -\frac{T_s}{C} & 1 \end{bmatrix},$$

$$B_{L,D} = B_L \cdot T_s = \begin{bmatrix} 0 & \frac{T_s}{C}\cdot I_L(k) \end{bmatrix}^T,\ C_{L,D} = C_L = \begin{bmatrix} 0 & 1 \end{bmatrix}$$

The design of a second order Luenberger observer is given by

$$\hat{x}_L(k+1) = A_{L,D} \cdot \hat{x}_L(k) + B_{L,D} \cdot \bar{u}(k) + H \cdot \bar{y}_L(k) \tag{19}$$

$$\hat{y}_L(k+1) = C_{L,D} \cdot \hat{x}_L(k+1) \tag{20}$$

where

$$\hat{x}_L(k) = \left[\hat{I}_o(k) \quad \hat{V}_o(k) \right]^T, \; H = \left[h_1 \quad h_2 \right]^T, \; \bar{y}_L(k) = y_L(k) - \hat{y}_L(k) = C_{L,D} \cdot \left(x_L(k) - \hat{x}_L(k) \right),$$

$$\bar{x}_L(k) = x_L(k) - \hat{x}_L(k)$$

The variables $\hat{I}_o(k)$, and $\hat{V}_o(k)$ are the estimated load current and output voltage, respectively. The matrix $H = [h_1 \; h_2]^T$ describes the constant observer gain which has to be verified. The term $\bar{y}_L(k)$ represents the error between the measured and the observed value of the output variable of the system, and $\bar{x}_L(k)$ represents the error between the state variables and the observed.

Taking into account the above equations

$$\hat{x}_L(k+1) = \left(A_{L,D} - H \cdot C_{L,D} \right) \cdot \hat{x}_L(k) + B_{L,D} \cdot \bar{u}(k) + H \cdot y_L(k) \tag{21}$$

Similarly the error between the state variables and the observed at instant $(k+1) \cdot T_s$ is

$$\bar{x}_L(k+1) = x_L(k+1) - \hat{x}_L(k+1) = (A_{L,D} - H \cdot C_{L,D}) \cdot \bar{x}_L(k) \tag{22}$$

The above error converges to zero if the observer is stable, at a rate determined by the eigenvalues of the matrix $[A_{L,D} - H \cdot C_{L,D}]$. If the pair $(A_{L,D}, C_{L,D})$ is observable, then given an arbitrary set of locations in the complex plane, the gain H exists which places the observer eigenvalues at these locations.

Therefore, the estimated variables $\hat{I}_o(k+1)$, $\hat{V}_o(k+1)$ considering the gain matrix H and are given by

$$\hat{V}_o(k+1) = (1 - h_1) \cdot \hat{V}_o(k) - \frac{T_s}{C} \cdot \hat{I}_o(k) + h_1 \cdot V_o(k) + \frac{T_s}{C} \cdot I_L(k) \cdot \bar{u}(k) \tag{23a}$$

$$\hat{I}_o(k+1) = \hat{I}_o(k) + h_2 \cdot (V_o(k) - \hat{V}_o(k)) \tag{23b}$$

Taking the above equations into account from now on, the estimated current $\hat{I}_o$ will be used instead the actual I_o.

Experimental results

For the experimental verification, a boost converter was built by using an IRF620 MOSFET and an MUR840 diode as switches. The control platform used was a standalone board, featuring a 16-bit floating point DSP (Experiment kit F28335 from Texas Instruments). The rated nominal input voltage $V_i = 20$ V, nominal output voltage $V_o = 25$ V, while the sampling time is $T_s = 20$ μs. The inductor value of the ferrite coil is $L = 0.6$ mH, the internal resistance of the inductor $R_L = 0.37$ Ohm and the filter capacitor value is $C = 220$ μF. The weighting factors of the constraints are defined as, $p_a = 3$ and $p_b = 0.01$, and the bounds of the errors, e, at $I_{L,max} = 1.1 \cdot I_L^*$, $I_{L,min} = 0.9 \cdot I_L^*$. The prediction horizon is $N = 3$.

Firstly the controller is tested under an output reference voltage step change from V_o^* = 25 V to V_o^* = 40 V, with a constant load R = 73 Ohm. The dynamic performance during the transition is further illustrated in Fig. 4, where the step change is shown in detail. The controller exhibits satisfactory transient characteristics, since it settles at the new operating point quickly and accurately.

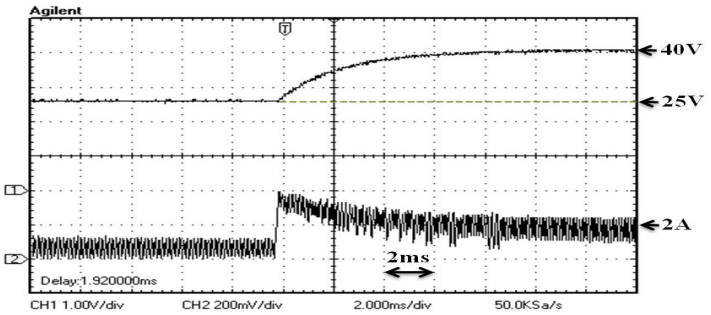

Fig. 4. Experimental results for the output voltage reference change from 25 V to 40 V. Channel 1, output voltage (probe x10), Channel 2 inductor current (current probe 100mV=>1A).

The second case to be analyzed is that of a ramp variation in the input voltage, during the previously attained point of operation (which means V_o = 40 V) from V_i = 20 V to V_i = 15.5 V. The segment of interest in this scenario is depicted in Fig. 5. As can been seen, the output voltage remains unaffected despite any disturbances in the input voltage, which are rejected by the controller.

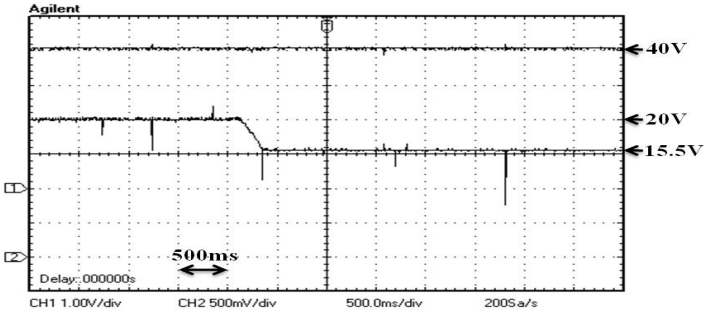

Fig. 5. Experimental results for a ramp variation in input voltage from 20 V to 15.5 V. Channel 1, output voltage (probe x10), Channel 2 input voltage (probe x10).

Furthermore, the robustness of the controller is tested under a load step change from R = 73 Ohm to R = 35 Ohm (Fig. 6), while the output voltage is kept at V_o = 40 V with the input voltage at V_i = 15.5 V. The experimental results show the fast response of the controller, while significant overshoots or undershoots are not observed at the output voltage.

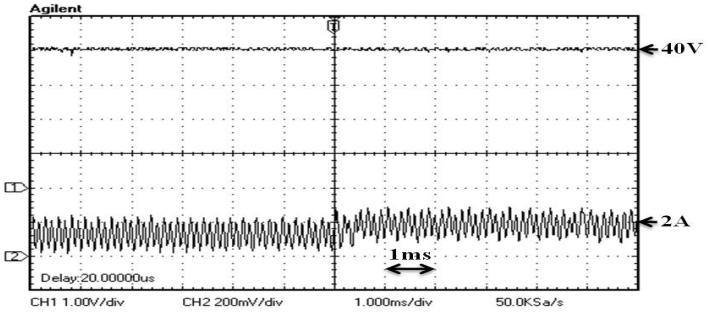

Fig. 6. Experimental results for a step variation in the load from 73 Ohm to 35 Ohm. Channel 1, output voltage (probe x10), Channel 2 inductor current (current probe 100mV=>1A).

Conclusion

In this paper a current model predictive control for dc-dc boost converters is proposed. The employed control method features a current controller, the robustness and very fast dynamic responses of which are its main benefits. Despite the fact that the converter is operating under variable switching frequency, the nature of the controller implies that it is directly extendable to other dc-dc converter topologies (for example the interleaved boost converter).

References

[1] J. M. Maciejowski: Predictive Control with Constraints, Prentice Hall publications, 2002.

[2] R. Möbus, M. Baotic, and M. Morari: Multi-Object Adaptive Cruise Control, Hybrid Systems: Computation and Control, vol. 2623, pp. 359-374, Lecture Notes in Computer Science, 2003.

[3] Cortes, J. Rodriguez, P. Antoniewicz, and M. Kazmierkowski: Direct Power Control of an AFE Using Predictive Control, IEEE Transactions on Power Electronics, vol. 23, No 5, pp. 2516-2523, Sep. 2008.

[4] J. Rodriguez, J. Pontt, C. A. Silva, P. Correa, P. Lezana, P. Cortes, and U. Ammann: Predictive Current Control of a Voltage Source Inverter, IEEE Transactions on Power Electronics, vol. 54, no 1, pp. 495-503, Feb. 2007.

[5] T. Geyer, G. Papafotiou, R. Frasca, and M. Morari: Constrained Optimal Control of the Step-Down DC-DC Converter, IEEE Transactions on Power Electronics, vol. 23, no 5, pp. 2454-2464, Sep. 2008.

[6] A. G. Beccuti, G. Papafotiou, R. Frasca, and M. Morari: Explicit Hybrid Model Predictive Control of the dc-dc Boost Converter, IEEE Power Electronics Specialist Conference PESC, Orlando, Florida, USA, pp. 2503-2509, June 2007.

[7] R. W. Erickson, D. Maksimovic: Fundamentals of Power Electronics, Kluwer Academic Publishers, 2nd edition, 2000.

[8] G. Th. Kostakis, S. N. Manias, and N. I. Margaris: A Generalized Method for Calculating the RMS Values of Switching Power Converters, IEEE Transactions on Power Electronics, vol. 15, no 4, pp. 616-625, July 2000.

[9] G. Pannocchia and J. B. Rawlings: Disturbance models for offset-free model-predictive control, AIChe Journal, vol. 49, no. 2, pp. 426-437, Feb. 2003.

[10] C. T. Chen: Linear System Theory and Design, Oxford University Press, 3rd edition, 1998.